Suppression of water-column multiples by combining components of OBS surveys

Yan Yan and R. James Brown

ABSTRACT

In ocean-bottom seismic data, multiples can be catalogued into pure water-column reverberations, receiver-side multiples, and source-side multiples. The multiples belonging to pure water-column reverberations and receiver-side reflections at the free surface are contained in the downgoing wavefield, while the primary reflections and pure source-side multiples are contained in the upgoing wavefield. Multiples containing bounces on both the source and receiver sides are considered receiver-side multiples for our purposes, since they arrive travelling downwards. Since the primary reflections are contained only in the upgoing wavefield, it is natural to consider a wavefield-separation technique.

The essence of wavefield decomposition techniques is to combine the pressure, the horizontal and vertical velocity components in proper proportions to obtain the upgoing and downgoing wavefields. With wavefield-separation techniques, the upgoing wavefield, without any receiver-side multiples, can be successfully extracted. After removal of the downgoing wavefield, however, source-side multiple energy remains as part of the upgoing wavefield. In laterally homogeneous cases, source-side multiples will have raypaths that are equivalent in length to those of corresponding receiver-side multiples. So the two types of multiple are recorded simultaneously. We exploit this circumstance to devise a method, based on cross-correlation, to further attenuate the source-side multiple energy.

INTRODUCTION

Multicomponent seafloor recording techniques have evolved continuously during the last decade and achieved promising results in the seismic exploration industry. Seafloor recording tools usually consist of a three-component (x, y, z directions) velocity-field measurement in the seafloor material and a pressure measurement in the water just above the bottom (e.g., Berg et al., 1994).

A serious problem in marine seismic data is that the measurements are contaminated by multiple reflections. Many schemes for combining data to obtain the demultipled datasets have been presented in the literature. According to Osen et al. (1999), three decades ago, White (1965) pointed out the possible usefulness to geophysical prospecting and oceanographic research of deploying a composite detector at the seafloor. His algorithm for attenuating water-column reverberations in the pressure recording is later reformulated and implemented by Barr and Sanders (1989), who designed the dual-sensor method to attenuate the downgoing waves.

Amundsen and Reitan (1994) pointed out how White's algorithm could be derived by wavefield separation – decomposing multicomponent seafloor recordings into upgoing and downgoing P and S waves. Several researchers (e.g., Osen et al., 1999;

Schalkwijk et al., 1999; etc) have worked on wavefield separation and have combined multicomponent data in different ways to lead to different wavefield-separation formulae for various applications.

Simply extracting the upgoing wavefield cannot eliminate the source-side water-column multiples or any multiples generated solely below the seafloor. In the case of lateral homogeneity, source-side multiples will have raypaths that are equivalent in length to those of corresponding receiver-side multiples, so the two types of multiples are recorded simultaneously. In vertical-geophone data, these two contributions can have comparable energies but opposite polarities, which partly attenuates the multiples by destructive interference before any wavefield separations (Brown and Yan, 1999). Then a source-side free-surface multiple would be stronger on the upgoing vertical-geophone trace after separation than on the actual recorded trace. Such strong source-side multiples in the upgoing wavefield need to be suppressed by other means.

This paper will analyze the downgoing multiple attenuation on each of three recorded components (pressure, vertical velocity, and inline velocity) using a wavefield-separation technique and describe how the source-side multiples can be further removed from the separated upgoing wavefield. Numerical data and real data examples are provided for illustration.

WAVEFIELD DECOMPOSITION THEORY

Since the recorded wavefield is composed of the waves in both water (above the seafloor) and elastic media (below the seafloor), the decomposition can be performed in water (acoustic decomposition) and in the elastic media (elastic decomposition).

Acoustic decomposition just above the sea floor

In water, the upgoing and downgoing pressure wavefields, U_P^W and D_P^W, can be computed from the pressure component and the vertical component of the particle velocity vector (Amundsen and Reitan, 1994) as:

$$U_P^W(z_1^-) = \frac{1}{2}\left[W(z_1^-) - \frac{\rho_1}{q_{\alpha 1}} V_z(z_1^-) \right], \tag{1}$$

and

$$D_P^W(z_1^-) = W(z_1^-) - U_P^W(z_1^-). \tag{2}$$

where $q_{\alpha_1} = \sqrt{(\alpha_1^{-2} - p^2)}$. Also, ρ_1 is the density of water, z_1^- denotes a depth just above the sea floor, and z_1^+ denotes a depth just below the sea floor. W is the pressure, and V_z is the vertical component of particle velocity; the subscript indicating the type of wave, and the superscript indicating the component type.

Elastic decomposition just below the sea floor

The wave equation can be expressed in the form of a first-order ordinary differential equation in stress and velocity (Aki and Richards, 1980):

$$\frac{d}{dz}\mathbf{B} = -i\omega\mathbf{A}\mathbf{B}, \tag{3}$$

where **B** is the vector that contains the stress and velocity variables across a plane elastic/elastic interface, and

$$\mathbf{B} = (V_z, S_x, S_y, S_z, V_x, V_y)^{\mathrm{T}}. \tag{4}$$

In equation (4), V_i are transformed components of particle velocity: V_x and V_y are horizontal components and V_z is the vertical component. S_z is the normal component of the traction in the solid, S_x and S_y are the shear components of the traction, z is depth, positive downward, and ω is angular frequency. **A** is the system matrix defined as:

$$\mathbf{A} = \begin{bmatrix} 0 & \mathbf{A_1} \\ \mathbf{A_2} & 0 \end{bmatrix}, \tag{5}$$

where

$$\mathbf{A_1} = \begin{bmatrix} \dfrac{1}{\lambda+2\mu} & \dfrac{\lambda p_1}{\lambda+2\mu} & \dfrac{\lambda p_2}{\lambda+2\mu} \\ \dfrac{\lambda p_1}{\lambda+2\mu} & \rho - \dfrac{4\mu(\lambda+\mu)p_1^2}{\lambda+2\mu} - \mu p_2^2 & -\dfrac{\mu(3\lambda+2\mu)p_1 p_2}{\lambda+2\mu} \\ \dfrac{\lambda p_2}{\lambda+2\mu} & -\dfrac{\mu(3\lambda+2\mu)p_1 p_2}{\lambda+2\mu} & \rho - \dfrac{4\mu(\lambda+\mu)p_1^2}{\lambda+2\mu} - \mu p_1^2 \end{bmatrix}, \tag{6}$$

and

$$\mathbf{A_2} = \begin{bmatrix} \rho & p_1 & p_2 \\ p_1 & \mu^{-1} & 0 \\ p_2 & 0 & \mu^{-1} \end{bmatrix}, \tag{7}$$

where λ and μ are the Lamé coefficients, p_1 and p_2 are horizontal slowness, i.e.,

$p_1 = k_1/\omega$, and $p_2 = k_2/\omega$. The p_1 and p_2 have to satisfy the relation:

$$p^2 = p_1^2 + p_2^2. \tag{8}$$

The wavefield separation can be obtained by eigendecomposition of the matrix **A**, i.e., $\mathbf{A} = \mathbf{L}^{-1}\,\mathbf{\Lambda}\,\mathbf{L}$, where **L** is the matrix composed of eigenvectors of matrix **A** and **Λ**

is the diagonal matrix composed of the eigenvalues of **A**. Then, equation (3) can be written as

$$\frac{d}{dz}\mathbf{B} = -i\omega\mathbf{L}^{-1}\mathbf{\Lambda}\mathbf{L}\mathbf{B}. \tag{9}$$

It can be shown that $\mathbf{\Lambda}$ can be written as:

$$\mathbf{\Lambda} = diag\left(q_P, q_{SV}, q_{SH}, -q_P, -q_{SV}, -q_{SH}\right). \tag{10}$$

The physical meaning of equation (10) is that eigenvalues q_P, q_{SV}, and q_{SH} correspond to the upgoing waves, whereas eigenvalues $-q_P$, $-q_{SV}$, and $-q_{SH}$ correspond to the downgoing waves. Therefore, equation (9) can be further decomposed into two equations that correspond to up- and downgoing waves, respectively, i.e.:

$$\frac{d}{dz}\mathbf{B}^U = -i\omega\mathbf{L}^{-1}\mathbf{\Lambda_1}\mathbf{L}\mathbf{B} \quad \text{and} \quad \frac{d}{dz}\mathbf{B}^D = -i\omega\mathbf{L}^{-1}\mathbf{\Lambda_2}\mathbf{L}\mathbf{B}, \tag{11}$$

where the superscripts *U* and *D* indicate upgoing and downgoing .

In order to solve equation (11), a boundary condition is needed. According to Aki and Richards (1980), at the boundary between two solid media in welded contact, the components of particle velocity (or displacement) and traction are continuous over the boundary. However, across the boundary between an in-viscid fluid and a solid (e.g. the ocean bottom), only the vertical component of the particle-velocity is continuous; the horizontal components of particle velocity can be discontinuous, implying that slip can occur parallel to the boundary. Further, the pressure in the fluid is equal to the negative of the vertical component of the traction in the solid, while the horizontal components of the traction in the solid vanish at the interface. So, at the seafloor, $z = z_1 + \varepsilon$ as $\varepsilon \to 0$, and we have:

$$\begin{gathered} S_x(z_1^+) = S_x(z_1^-) = 0;\ S_y(z_1^+) = S_y(z_1^-) = 0; \\ S_z(z_1^+) = -W(z_1^-); \text{and } V_z(z_1^+) = V_z(z_1^-), \end{gathered} \tag{12}$$

where, z_1^- denotes a depth just above the seafloor, and z_1^+ denotes a depth just below the seafloor.

Moreover, in the system of equations (3), all the types of wave (P, SV, and SH) are included. We can obtain plane P-SV waves when $S_y = V_y = 0$ and $p_2 = 0$, and obtain SH waves when $S_x = S_z = V_x = V_z = 0$ and p_1=0. We can also obtain the plane P waves when $S_x = S_y = V_x = V_y = 0$ and $p_1 = p_2 = 0$ (Gilbert and Backus, 1966). Therefore, the upgoing and downgoing wavefields for P, SV and SH just below the seafloor can be obtained correspondingly from equation (11).

Following the derivation given by Amundsen and Reitan (1994), we have the upgoing and downgoing P- and S-wave vertical traction components:

$$U_P^{Sz}(z_1^+) = \frac{1}{2}(1-2p^2\beta_2^2)S_z(z_1^+) + \frac{\rho_2}{2q_{\alpha 2}}(1-2p^2\beta_2^2)^2 V_z(z_1^+) + ip\mu_2(1-2p^2\beta_2^2)V_r(z_1^+)$$

$$D_P^{Sz}(z_1^+) = \frac{1}{2}(1-2p^2\beta_2^2)S_z(z_1^+) - \frac{\rho_2}{2q_{\alpha 2}}(1-2p^2\beta_2^2)^2 V_z(z_1^+) + ip\mu_2(1-2p^2\beta_2^2)V_r(z_1^+)$$

$$U_S^{Sz}(z_1^+) = (p\beta_2)^2 S_z(z_1^+) + 2(p\beta_2)^2\mu_2 q_{\beta_2} V_z(z_1^+) - ip\mu_2(1-2p^2\beta_2^2)V_r(z_1^+) \tag{13}$$

$$D_S^{Sz}(z_1^+) = (p\beta_2)^2 S_z(z_1^+) - 2(p\beta_2)^2\mu_2 q_{\beta_2} V_z(z_1^+) - ip\mu_2(1-2p^2\beta_2^2)V_r(z_1^+),$$

where α_2, the P-wave velocity in the solid, and β_2, the S-wave velocity in the solid, are defined as:

$$\alpha_2 = \sqrt{\lambda + 2\mu} \quad \text{and} \quad \beta_2 = \sqrt{\mu/\rho_2}, \tag{14}$$

ρ_2 is the density in the solid, λ and μ are the Lamé coefficients. The vertical ray parameters are defined as:

$$q_{\alpha_2} = \sqrt{\alpha_2^{-2} - p^2}, \; q_{\beta_2} = \sqrt{\beta_2^{-2} - p^2}. \tag{15}$$

The upgoing and downgoing P- and S-wave vertical particle-velocity components are:

$$U_P^{V_z}(z_1^+) = \frac{q_{\alpha 2}}{2\rho_2} S_z(z_1^+) - \frac{1}{2}(1-2p^2\beta_2^2) V_z(z_1^+) - ip\beta_2^2 q_{\alpha 2} V_r(z_1^+)$$

$$D_P^{V_z}(z_1^+) = -\frac{q_{\alpha 2}}{2\rho_2} S_z(z_1^+) + \frac{1}{2}(1-2p^2\beta_2^2) V_z(z_1^+) - ip\beta_2^2 q_{\alpha 2} V_r(z_1^+)$$

$$U_S^{V_z}(z_1^+) = -\frac{p^2}{2\rho_2 q_{\beta_2}} S_z(z_1^+) - (p\beta_2)^2 V_z(z_1^+) + \frac{ip}{q_{\beta_2}}(1-2p^2\beta_2^2) V_r(z_1^+) \tag{16}$$

$$D_S^{V_z}(z_1^+) = -\frac{p^2}{2\rho_2 q_{\beta_2}} S_z(z_1^+) + (p\beta_2)^2 V_z(z_1^+) + \frac{ip}{q_{\beta_2}}(1-2p^2\beta_2^2) V_r(z_1^+).$$

The upgoing and downgoing P- and S-wave horizontal particle-velocity components are:

$$U_P^{V_r}(z_1^+) = -\frac{ip}{2\rho_2} S_z(z_1^+) - \frac{ip}{2q_{\alpha 2}}(1-2p^2\beta_2^2) V_z(z_1^+) + (p\beta_2)^2 V_r(z_1^+)$$

$$D_P^{V_r}(z_1^+) = -\frac{ip}{2\rho_2} S_z(z_1^+) + \frac{ip}{2q_{\alpha 2}}(1-2p^2\beta_2^2) V_z(z_1^+) + (p\beta_2)^2 V_r(z_1^+)$$

$$U_S^{V_r}(z_1^+) = \frac{ip}{2\rho_2} S_z(z_1^+) + ip\beta_2^2 q_{\beta_2} V_z(z_1^+) + \frac{1}{2}(1-2p^2\beta_2^2) V_r(z_1^+) \tag{17}$$

$$D_S^{V_r}(z_1^+) = \frac{ip}{2\rho_2} S_z(z_1^+) - ip\beta_2^2 q_{\beta_2} V_z(z_1^+) + \frac{1}{2}(1-2p^2\beta_2^2) V_r(z_1^+).$$

The above decomposition procedure for separating multicomponent ocean-bottom data into up- and downgoing P and S waves is proposed by Amundsen and Reitan (1994). Their derivation is based on the assumption that the Earth consists of homogeneous plane layers and that axial symmetry applies. Assuming that the fields are recorded along a line at the seafloor, they used the Fourier-Bessel transform for obtaining the decomposition formulae in the slowness domain (Osen et al., 1999). Following the investigation of Osen et al., (1999), we will describe the corresponding elastic decomposition formulae for each component with the assumption that the seafloor is locally flat, with constant medium parameters. The Fourier transform is applied in a Cartesian coordinate system.

WAVEFIELD DECOMPOSITION OF EACH COMPONENT

If we rewrite Amundsen and Reitan's (1994) decomposition equations, (13), (16), and (17) in Cartesian coordinates, then we have the following decomposition

equations for each of the components (hydrophone, vertical, inline and crossline geophones).

Pressure component

The upgoing and downgoing P- and S-wavefield decomposition formulae for the vertical traction component (after Amundsen and Reitan, 1994; Osen et al., 1999):

$$
\begin{aligned}
U_P^{S_z} &= \frac{1}{2}(1-2p^2\beta_2^2)S_z + \frac{\rho_2}{2q_{\alpha 2}}(1-2p^2\beta_2^2)^2 V_z - \rho_2\beta_2^2(1-2p^2\beta_2^2)(p_1V_x + p_2V_y),\\
D_P^{S_z} &= \frac{1}{2}(1-2p^2\beta_2^2)S_z - \frac{\rho_2}{2q_{\alpha 2}}(1-2p^2\beta_2^2)^2 V_z - \rho_2\beta_2^2(1-2p^2\beta_2^2)(p_1V_x + p_2V_y),\\
U_{SV}^{S_z} &= (p\beta_2)^2 S_z + 2(p\beta_2)^2\mu_2 q_{\beta_2} V_z + \rho_2\beta_2^2(1-2p^2\beta_2^2)(p_1V_x + p_2V_y),\\
D_{SV}^{S_z} &= (p\beta_2)^2 S_z - 2(p\beta_2)^2\mu_2 q_{\beta_2} V_z + \rho_2\beta_2^2(1-2p^2\beta_2^2)(p_1V_x + p_2V_y),
\end{aligned}
\tag{18}
$$

such that

$$S_z = U_P^{S_z} + D_P^{S_z} + U_{SV}^{S_z} + D_{SV}^{S_z}. \tag{19}$$

After using the boundary condition in system equations (12): $S_z(z_1^+) = -W(z_1^-)$, The equation (19) can be expressed as

$$W = U_P^W + D_P^W + U_{SV}^W + D_{SV}^W, \tag{20}$$

forming the two sums:

$$U^W = U_P^W + U_{SV}^W, \tag{21}$$

and

$$D^W = D_P^W + D_{SV}^W. \tag{22}$$

Then, the system of equations (18) can be rewritten as a matrix equation:

$$
\begin{pmatrix} U^W \\ D^W \end{pmatrix} = \frac{1}{2}\begin{pmatrix} 1 & -\left(\frac{\rho}{q_\alpha}[(1-2p^2\beta^2)^2 + 4p^2\beta^4 q_\alpha q_\beta\right) \\ 1 & \frac{\rho}{q_\alpha}[(1-2p^2\beta^2)^2 + 4p^2\beta^4 q_\alpha q_\beta \end{pmatrix}\begin{pmatrix} W \\ V_z \end{pmatrix}, \tag{23}
$$

The upgoing wavefield (summing P and S waves) for the pressure component can be obtained using the formula below:

$$U^{W}(z_1^+) = \frac{1}{2}\left\{W(z_1^-) - \frac{\rho}{q_\alpha}\left[(1-2p^2\beta^2)^2 + 4p^2\beta^4 q_\alpha q_\beta\right]V_z(z_1^+)\right\}. \qquad (24)$$

Vertical particle-velocity component

The upgoing and downgoing P- and S-wavefield decomposition formulae for the vertical particle-velocity component (after Amundsen and Reitan, 1994; Osen et al., 1999) are:

$$\begin{aligned}
U_P^{V_z} &= \frac{q_{\alpha 2}}{2\rho_2}S_z - \frac{1}{2}(1-2p^2\beta_2^2)V_z + \beta_2^2 q_{\alpha 2}(p_1V_x + p_2V_y)\\
D_P^{V_z} &= -\frac{q_{\alpha 2}}{2\rho_2}S_z + \frac{1}{2}(1-2p^2\beta_2^2)V_z + \beta_2^2 q_{\alpha 2}(p_1V_x + p_2V_y)\\
U_{SV}^{V_z} &= -\frac{p^2}{2\rho_2 q_{\beta_2}}S_z - (p\beta_2)^2 V_z - \frac{1}{2q_{\beta_2}}(1-2p^2\beta_2^2)(p_1V_x + p_2V_y)\\
D_{SV}^{V_z} &= -\frac{p^2}{2\rho_2 q_{\beta_2}}S_z + (p\beta_2)^2 V_z - \frac{1}{2q_{\beta_2}}(1-2p^2\beta_2^2)(p_1V_x + p_2V_y),
\end{aligned} \qquad (25)$$

such that

$$V_z = U_P^{V_z} + D_P^{V_z} + U_{SV}^{V_z} + D_{SV}^{V_z}. \qquad (26)$$

Using similar strategy for the pressure component, we can get the upgoing wavefield (summing P and S waves) for the vertical-geophone component as follows:

$$U^{V_z}(z_1^+) = \frac{1}{2}\left\{V_z(z_1^+) + \left[1-2\beta^2(p^2+q_\alpha q_\beta)\right]\left[\frac{p_1}{q_\beta}V_x(z_1^+) + \frac{p_2}{q_\beta}V_y(z_1^+)\right] - \frac{1}{\rho q_\beta}(p^2+q_\alpha q_\beta)W(z_1^-)\right\}. \qquad (27)$$

Inline particle-velocity component

The upgoing and downgoing P- and S-wavefield decomposition formulae for the inline particle-velocity component (after Amundsen and Reitan, 1994; Osen et al., 1999) are:

$$\begin{aligned}
U_P^{V_x} &= -\frac{p_1}{2\rho_2}S_z - \frac{p_1}{2q_{\alpha 2}}(1-2p^2\beta_2^2)V_z + (p_1\beta_2)^2(p_1V_x + p_2V_y)\\
D_P^{V_x} &= -\frac{p_1}{2\rho_2}S_z + \frac{p_1}{2q_{\alpha 2}}(1-2p^2\beta_2^2)V_z + (p_1\beta_2)^2(p_1V_x + p_2V_y)
\end{aligned}$$

$$U_S^{V_r} = \frac{p_1}{2\rho_2} S_z + p_1 \beta_2^2 q_{\beta_2} V_z + \frac{p_1}{2p^2}(1-2p^2\beta_2^2)(p_1 V_x + p_2 V_y) \tag{28}$$

$$D_S^{V_r} = \frac{p_1}{2\rho_2} S_z - p_1 \beta_2^2 q_{\beta_2} V_z + \frac{p_1}{2p^2}(1-2p^2\beta_2^2)(p_1 V_x + p_2 V_y)$$

$$U_{SH}^{V_x} = D_{SH}^{V_x} = \frac{p_2}{2p^2}(p_1 V_x - p_2 V_y),$$

such that

$$V_x = U_P^{V_x} + D_P^{V_x} + U_S^{V_r} + D_S^{V_r} + U_{SH}^{V_x} + D_{SH}^{V_x}. \tag{29}$$

The upgoing wavefield (summing P and S waves) for the inline geophone component is given by:

$$U^{V_x}(z_1^+) = \frac{1}{2}\left\{ V_x(z_1^+) - \frac{p_1}{q_\alpha}\left[1 - 2\beta^2(p^2 + q_\alpha q_\beta)\right] V_z(z_1^+) \right\}. \tag{30}$$

Crossline particle-velocity component

The upgoing and downgoing P- and S-wavefield decomposition formulae for the crossline particle-velocity component (after Amundsen and Reitan, 1994; Osen et al., 1999) are:

$$U_P^{V_y} = -\frac{p_2}{2\rho_2} S_z - \frac{p_2}{2q_{\alpha 2}}(1-2p^2\beta_2^2) V_z + (p_2\beta_2)^2 (p_1 V_x + p_2 V_y)$$

$$D_P^{V_y} = -\frac{p_2}{2\rho_2} S_z + \frac{p_2}{2q_{\alpha 2}}(1-2p^2\beta_2^2) V_z + (p_2\beta_2)^2 (p_1 V_x + p_2 V_y)$$

$$U_{SV}^{V_y} = \frac{p_2}{2\rho_2} S_z + p_2 \beta_2^2 q_{\beta_2} V_z + \frac{p_2}{2p^2}(1-2p^2\beta_2^2)(p_1 V_x + p_2 V_y) \tag{31}$$

$$D_{SV}^{V_y} = \frac{p_2}{2\rho_2} S_z - p_2 \beta_2^2 q_{\beta_2} V_z + \frac{p_2}{2p^2}(1-2p^2\beta_2^2)(p_1 V_x + p_2 V_y)$$

$$U_{SH}^{V_y} = D_{SH}^{V_x} = \frac{p_1}{2p^2}(p_2 V_x - p_1 V_y),$$

such that

$$V_y = U_P^{V_y} + D_P^{V_y} + U_{SV}^{V_y} + D_{SV}^{V_y} + U_{SH}^{V_y} + D_{SH}^{V_x}. \tag{32}$$

The upgoing wavefield (summing P and S waves) for crossline geophone component is:

$$U^{V_y}(z_1^+) = \frac{1}{2}\left\{V_y(z_1^+) - \frac{p_2}{q_\alpha}\left[1 - 2\beta^2(p^2 + q_\alpha q_\beta)\right]V_z(z_1^+)\right\}. \tag{33}$$

After applying equations (24), (27), (30) and (33), the upgoing wavefields for the four components can be obtained separately.

Now we look at equation (24) again, noting that only pressure and vertical velocity components are involved in this equation. We can also see that the upgoing wavefield for pressure can be obtained just by combining the pressure and scaled vertical particle-velocity components. We can also see that the pressure wavefield and the vertical velocity wavefield can be expressed by each other. This demultiple scheme just uses a scaling relationship between the two components.

If we rewrite this scaling relationship using the reflection coefficient of the seafloor, we have

$$U^W(z_1^+) = \frac{1}{2}\left\{W(z_1^-) - \frac{\rho_w c}{\cos\theta}\frac{(1+r)}{(1-r)}V_z(z_1^+)\right\}. \tag{34}$$

This is actually the dual-sensor method (Barr and Sanders, 1989). Therefore, we can take this method as a kind of wavefield-decomposition technique.

SOURCE-SIDE MULTIPLE SUPPRESSION

After application of our wavefield-separation technique, given above, the upgoing wavefield can be obtained and downgoing multiples, such as the direct wave, receiver-side multiples and reverberations, are sufficiently suppressed. However, the source-side multiples, being upgoing arrivals, are still left there. This kind of multiple has energy comparable to that of the primaries and they need to be further suppressed.

Source-side multiple identification

The scheme for attenuating the upgoing multiples has been presented by many researchers. Weglein et al. (1997) introduced a multiple suppression method by expanding the wavefield into a Born series. Each term of this series corresponds to a particular scattering path. If the terms corresponding to multiples in the forward series can be characterized, described and distinguished from the terms corresponding to the primaries, then suppression of multiples can be realized in the inverse series by removing those terms corresponding to multiples. Using a similar technique, Berkhout (1982) presented an adaptive filter method. However, application of these methods needs more theoretical research. Here, a simple means toward this end is the cross-correlation method.

It is known that the source-side multiple arrives from below and the receiver-side multiple arrives from above. These two contributions, from source and receiver sides,

are comparable in energy with opposite polarities for the vertical-component geophone. A simple way to identify them is calculate the cross-correlation values of upgoing wavefield data and downgoing wavefield data for the vertical-component geophone using this expression:

$$\psi_{UD}(j) = \frac{\sum_{i=1}^{L} U_{i+j} D_i}{\sqrt{\sum_{i=1}^{L} U_{i+j}^2 \sum_{i=1}^{L} D_i^2}}, \tag{35}$$

where, $\psi_{UD}(j)$ is the cross-correlation of the upgoing wavefield data, U, and the downgoing wavefield data, D, in each window. L is the length of the window, j is number of samples of a lag. In view of the identical arrival times (assuming lateral homogeneity) we focus our attention at zero-lag. Then the cross-correlation coefficients at samples where the source side multiples appear should approach –1, depending on how close to equality the amplitudes are of the upgoing and downgoing contributions to the multiple. Such large negative values can be used as indicators of source-side multiple energy. The indicated sample positions of source-side multiples on the vertical geophone can in turn be used to identify the positions of multiples in the upgoing wavefields of all the components.

Source-side multiple elimination

After the positions of the source-side multiples are identified on each of components, we can extract them and then subtract from the upgoing wavefields. However, if primary and multiple arrivals overlap, this simple subtraction also eliminates the primary information. So the best way to do it is to isolate these multiples from the *downgoing* wavefield (*no primaries*), scaling them, and then subtracting from the upgoing wavefields.

ESTIMATION OF ELASTIC PARAMETERS

Decomposition equations (24), (27), (30) and (33) all require an estimate of the elastic parameters of the sea materials. Estimation of seafloor wave propagation can be performed by amplitude-versus-offset (AVO) analysis (Amundsen and Reitan, 1995). Schalkwijk et al., (1999) also presented a method of estimating the elastic parameters by a two-step wavefield decomposition method. In their scheme, instead of going from the measured data directly to the end result – up and downgoing P and S waves – they use several intermediate decomposition results before coming to the final result and each intermediate result allows for the estimation of some unknown parameters.

Using a similar technique, Osen et al., (1999) performed the estimation of elastic parameter by applying equations (24), (27), (30) and (33) to the transmitted direct wave. Assuming that no upgoing waves interfere with the transmitted direct wave within a certain time window and offset range, they estimate the seafloor parameters from equations (24), (27), (30) and (33) by requiring that upgoing wavefield $U = 0$.

For equation (24), when a single plane-wave propagates directly from the source to the receiver in a direction perpendicular to a horizontal sea bottom, this equation can be written as:

$$U^W(z_1^+) = \frac{1}{2}\left[W(z_1^-) - \rho\alpha V_3(z_1^+)\right] \tag{36}$$

The scaling factor between the pressure and vertical velocity in equation (36) equals the P-wave impedance of the seafloor materials ($\rho\alpha$). By comparing the zero-offset trace for the direct wave on the hydrophone with the corresponding trace for the direct wave on the vertical geophone, an estimate of the impedance, $\rho\alpha$, can be obtained.

To test this strategy, we modelled the pressure and vertical-velocity traces recorded at the acoustic/elastic interface in a model between a water layer and a semi-infinite half-space with elastic parameters α=2100m/s, β=700m/s and ρ=2.098g/cm^3. The explosive point source was placed at 5m depth and the thickness of the water was set to 500m. When source depth is small compared to the water-layer thickness, the effect of the source ghost does not degrade the analysis (Osen et al., 1999).

Figure 1 shows the direct wave on the zero-offset pressure (W) trace, while the corresponding direct-wave arrival on the vertical velocity (V_3) trace is shown in Figure 2.

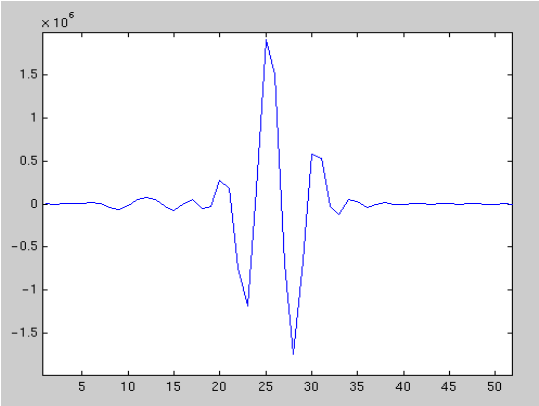

FIG. 1. The zero-offset trace for the direct wave on the hydrophone.

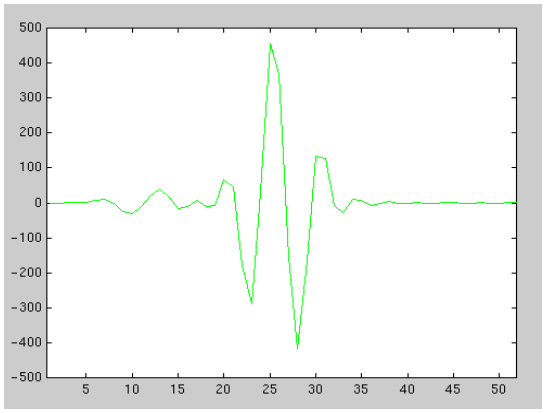

FIG. 2. The zero-offset trace for the direct wave on the vertical geophone.

For estimating the value of impedance, $\rho\alpha$, from equation (36), we require the upgoing wavefield, U, to vanish. Then we have

$$W(z_1^-) = \rho\alpha V_3(z_1^+) \tag{37}$$

By comparing the zero-offset trace for the direct wave on the hydrophone (Figure 1) with the corresponding trace for the direct wave on the vertical geophone (Figure 2), we obtain the estimated value of the impedance $\rho\alpha$=4.395. Comparing with the real parameters used for generating the synthetic data, for which $\rho\alpha$=4.4058, it shows excellent agreement. We can conclude that this method of estimation is sound.

We also illustrate this good agreement. Figure 3 shows the scaled geophone trace after using the estimated value of impedance as the scaling factor.

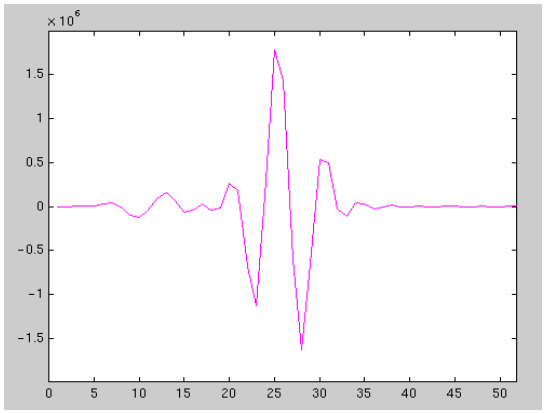

FIG. 3. The scaled vertical-velocity trace.

When we plot the synthetic zero-offset pressure trace, zero-offset vertical-velocity trace, and the $\rho\alpha$-scaled vertical-velocity trace together (Figure 4), we can see that the vertical-velocity trace has very small amplitude compared with that of the pressure trace. After using the estimated value of impedance as the scaling factor, they have the almost same amplitude. It demonstrates again that the medium parameter estimation is very good.

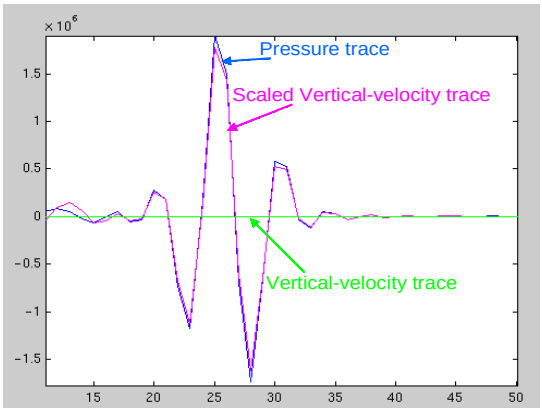

FIG. 4. Superposition of pressure trace, vertical-geophone trace and scaled vertical-geophone trace.

For further estimating other elastic parameters, we can use the estimated P-wave impedance, $\rho\alpha$, as a constraint in minimizing the equations (27), (30) and (33) with respect to the elastic parameters (or requiring that U=0), in a window containing the direct wave at a specific offset.

SYNTHETIC DATA EXAMPLES

To test the performance of equations (24), (27), (33) and (35), we use synthetic seismograms modelled in a plane-layered medium. This is a 2-D model with a 500m water layer and two further reflectors at depths of 750m and 900m. P-wave velocities are 1500m/s, 1900m/s and 2400m/s, in layers 1, 2 and 3, respectively. The synthetic data are generated by ELMO, an elastic modelling program based on the phase-shift-cascade method (Silawongsawat and Margrave, 1998). The synthetic pressure, vertical-velocity, and horizontal-velocity gathers are shown in Figures 5, 6 and 7, respectively. Note that primaries are present for events at approximately 0.59 and 0.72s. The downgoing direct arrival and its reverberations are present for events at approximately 0.33, 1.01 and 1.67s, respectively. Also notice that source-side multiples arrive at approximately 1.27s.

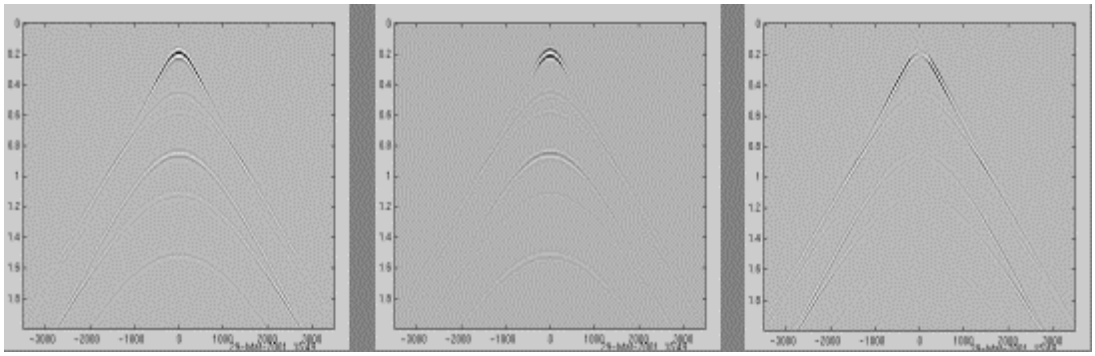

FIG. 5. Modelled total wavefield for hydrophone.

FIG. 6. Modelled total wavefield for vertical geophone.

FIG. 7. Modelled total wavefield for radial geophone.

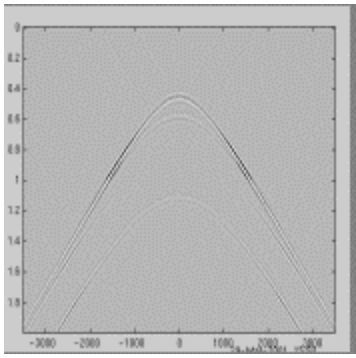

FIG. 8. Decomposed upgoing hydrophone wavefield.

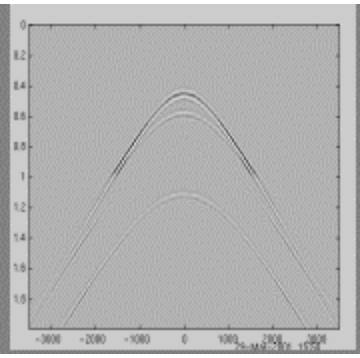

FIG. 9. Decomposed upgoing vertical-geophone wavefield.

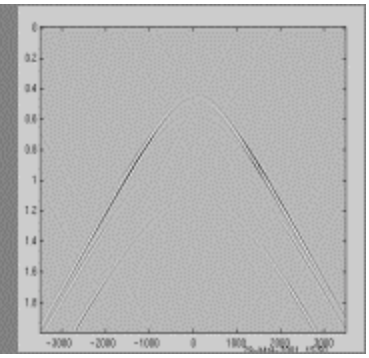

FIG. 10. Decomposed upgoing inline-geophone wavefield.

After application of our wavefield-separation equations (24), (27) and (33), the upgoing wavefields for each component are shown in Figures 8, 9 and 10. Comparing these with Figures 5, 6 and 7, we can see that the multiples belonging to downgoing waves are successfully suppressed. However, the source-side multiple still exists in the upgoing wavefields.

After applying the cross-correlation method [equation (35)], this multiple is sufficiently suppressed and the final upgoing wavefields are shown in Figures 11, 12 and 13, respectively, where only the primaries are preserved.

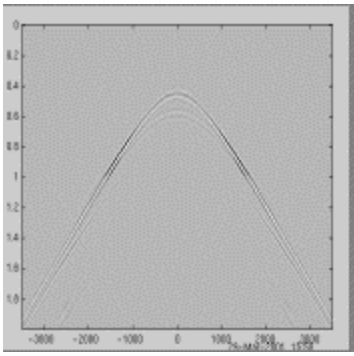

FIG. 11. Eliminating source-side multiple (hydrophone).

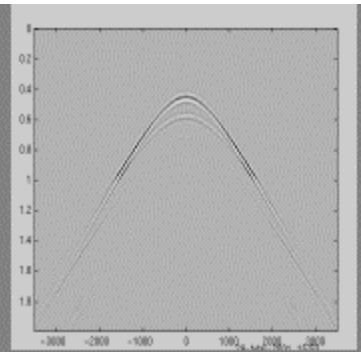

FIG. 12. Eliminating source-side multiple (vertical geophone).

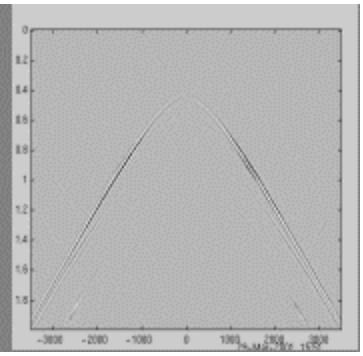

FIG. 13. Eliminating source-side multiple (inline geophone).

REAL DATA EXAMPLES

The wavefield decomposition for multicomponent ocean-bottom data works nicely on synthetic data provided that all the information about the elastic medium is known accurately. However, in real application, this information may not be known and due to measurement imperfections (different coupling, impulse response, etc.), this method is difficult to apply for field data.

OBS seismic data has been acquired over the Mahogany Field in the Gulf of Mexico and resampled at 4ms. The group interval was 25m. The water depth at the Mahogany field is about 120m, so the water-column reverberation period is about 160ms. The data quality is not good and there is a serious multiple problem.

Polarity determination

Before processing, we should decide whether the datasets have normal or reverse polarity. How do we ensure this? Brown (1999) gives detailed guidelines. According to him, to ensure positive or normal polarity for the vertical (Z) component, the direct downgoing P should have positive onsets. For normal polarity on the hydrophone (W) component, the direct P should then have negative onsets. For normal polarity on the inline (X) component, the direct P should have positive onsets. This normally means flipping X polarity for negative offsets. The crossline component should be treated in basically the same way as the inline component (Brown, 1999).

Figure 14 shows the vertical-component common-receiver gather. The first breaks, due to direct downgoing P, are seen at zero-offset at about 65ms. This arrival has a positive break. For the hydrophone-component common-receiver gather shown in Figure 15, the direct P should then have negative break. Figure 16 shows the inline-component common-receiver gather. We can see that positive-offset traces and negative-offset traces have the opposite polarity. After flipping polarity for negative offsets, we can see that the direct P wave now has a positive break for all offsets (Figure 17).

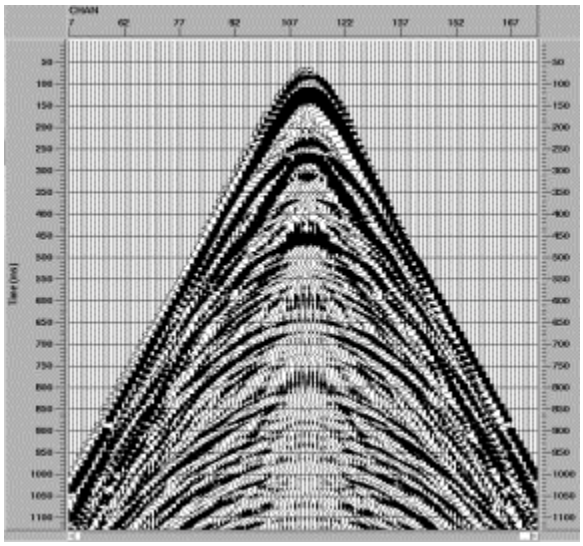

FIG. 14. A vertical-component common-receiver gather from Mahogony.

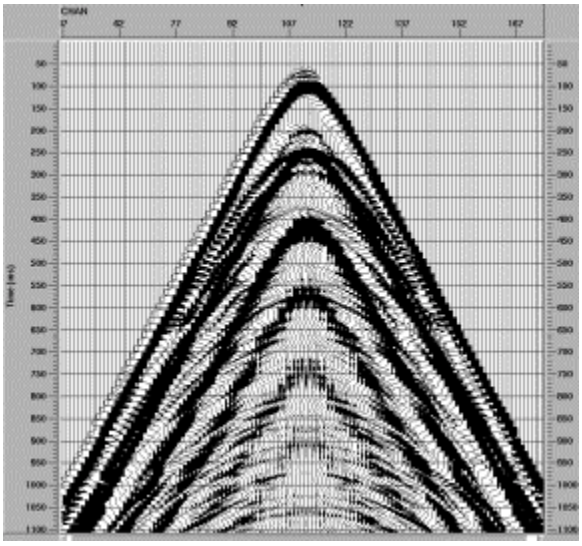

FIG. 15. A hydrophone-component common-receiver gather from Mahogony.

From Figure (14), (15) and (17), we can see this is very noisy dataset. The water-column reverberation arriving after the direct arrival, and those multiples associated with primary reflections, contaminate the whole section. Primary events are difficult to identify on both hydrophone data and geophone data.

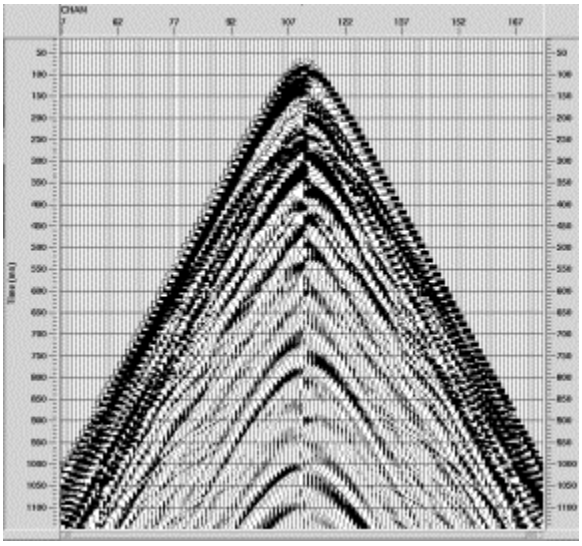

FIG. 16. An inline-component common-receiver gather from Mahogony. Positive-offset traces have the opposite polarity to that of negative-offset traces.

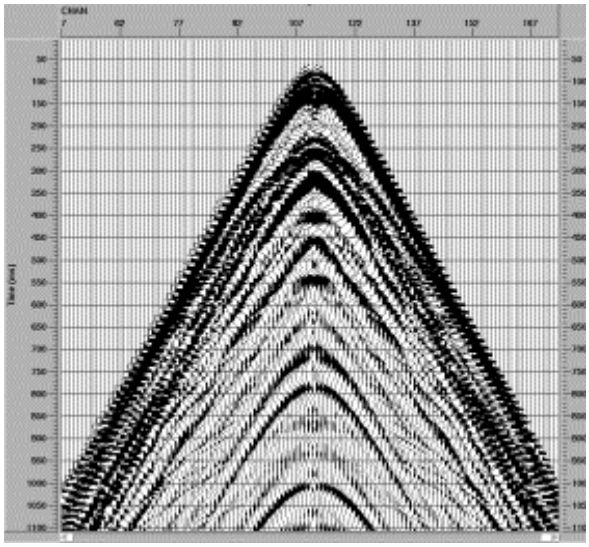

FIG. 17. The inline-component common-receiver gather, (Figure 16), after flipping polarity for negative offsets. Note that the negative offsets are on the right.

Calibration between hydrophone and vertical geophone

After deciding the polarities, the next step is to resolve the calibration relationship between the hydrophone and vertical geophone. Ball and Corrigan (1996) proposed that a match filter should be applied to the geophone trace to compensate for the different coupling and noise effects on the hydrophone and geophone trace. According to them, this match filter is estimated from the cross-ghosted traces. Cross-ghosted traces are the traces that result by applying the hydrophone ghost to the geophone traces, and the geophone ghost to the hydrophone traces. The primary and multiple trains of cross-ghosted traces should be the same, so cross-ghosted traces can be used to obtain the match filter. However the original traces cannot be used.

Schalkwijk et al. (1999) also proposed another scheme to determined the calibration between the pressure and vertical velocity components. They add the calibration filter λ into the acoustic decomposition equation (1), which becomes:

$$U_P^W(z_1^-) = \frac{1}{2}\left[W(z_1^-) - \lambda \frac{\rho_1}{q_{\alpha 1}} V_z(z_1^-) \right]. \tag{38}$$

The acoustic medium parameters are known, the condition for solving for λ is that the data should be windowed to exclude the primaries reflections (Schalkwijk et al., 1999).

Using the scheme described by Schalkwijk et al., (1999), setting the P-wave velocity of water to 1500m/s and the density of water to 1000kg/m^3 in equation (38), we obtain the scalar number for calibration between the hydrophone (Figure 14) and vertical geophone (Figure 15): $\lambda = 0.0021$.

Estimation of seafloor medium parameters

The wavefield-decomposition technique requires the seafloor medium parameters as input, so these should be known. For estimating the seafloor parameters from our real data, we applied the strategy described earlier and obtained: α=1900m/s, β=550m/s, ρ=2018.9kg/m^3.

Figure 18 shows the hydrophone trace (solid line) at 25m offset with the scaled vertical-geophone trace (dash-dot line) for the optimal estimate: α=1900m/s, β=550m/s, and ρ=2018.9kg/m^3. Figure 19 shows the inline trace (dash-dot line) for a 50m offset and the scaled vertical-geophone trace (solid line) for the optimal estimates.

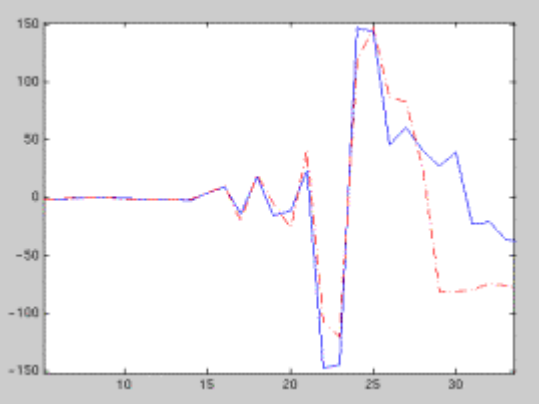

FIG. 18. Comparison of the direct wave arrival at 25m offset on the pressure trace (solid line) and the scaled vertical-velocity trace (dash-dot line) for the optimal estimates: α = 1900m/s, β = 550m/s, and ρ = 2018.9kg/m^3.

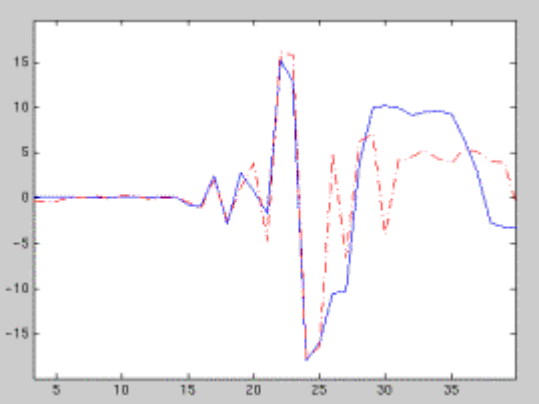

FIG. 19. Comparison of the direct wave arrival at 50m offset on the inline-velocity trace (dash-dot line) and the scaled vertical-velocity trace (solid line) for the optimal estimates: α=1900m/s, β = 550m/s, and ρ = 2018.9kg/m^3.

Decomposition results

After determining the dataset polarities, solving for the calibration between hydrophone and vertical geophone, and estimating the seafloor medium parameters,

the receiver gathers shown in Figures 14, 15 and 17 are then processed using our decomposition technique [equations (24), (27) and (30)]. The decomposed upgoing wavefields for the three components are shown in Figures 20 to 22, respectively.

Comparing with the input data shown in Figures 14, 15 and 17, the strong water-column reverberations arriving after the direct arrival at times around 100ms, 260ms, 420ms, 580ms, etc., are attenuated, while the primaries at times around 650ms, 820ms and 960ms show better resolution and continuity and can be observed quite confidently.

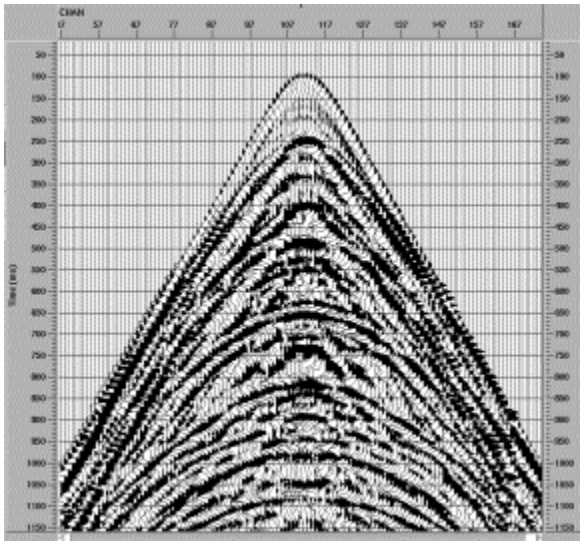

FIG. 20. Decomposed upgoing wavefield for vertical geophone component.

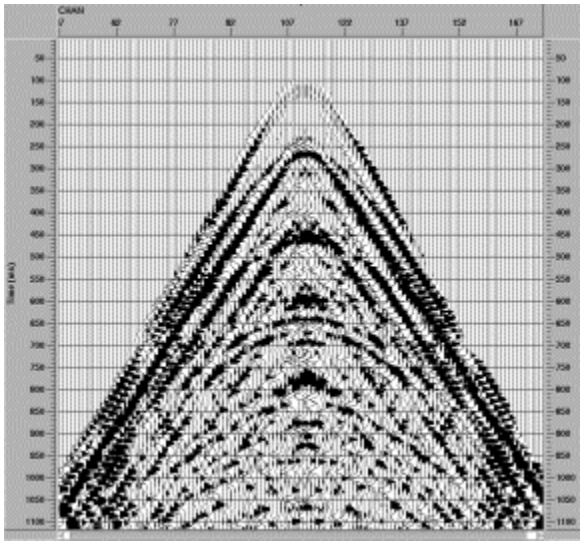

FIG. 21. Decomposed upgoing wavefield for hydrophone component.

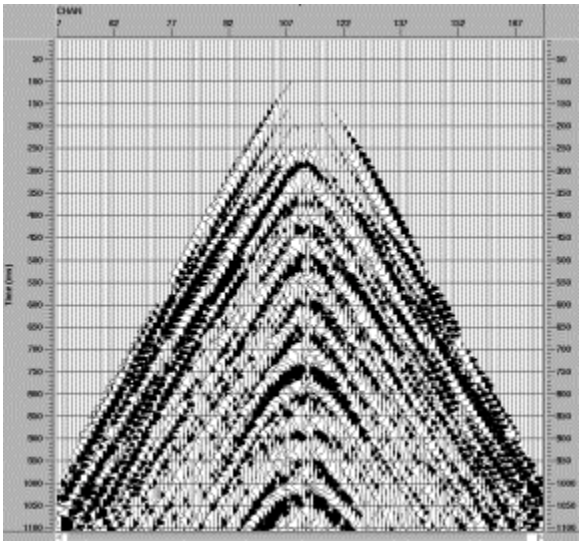

FIG. 22. Decomposed upgoing wavefield for inline-geophone component.

DISCUSSION

The wavefield decomposition technique is a fairly straightforward method applied to remove the receiver ghost and the accompanying reverberations in the water layer for OBC data. It does not require information about the source signature. Moreover, the decomposition can be performed without *a priori* knowledge of the medium parameters below the ocean-bottom. An assumption in this method is that the recording surface is locally flat with constants medium parameters. Synthetic and real examples illustrated the successful application of this algorithm.

According to the difference of wave propagation paths, seismic waves can be grouped into downgoing and upgoing wavefields. The downgoing wavefield contains the direct wave, water-column reverberations, and receiver-side ghosts (Figure 23); while the upgoing wavefield contains all the primaries and free-surface multiples (source-side multiples, internal multiples) (Figure 24). Using the wavefield decomposition method, the output is the upgoing wavefield. So it will not totally remove the effect of the free surface as does the inverse-scattering series method presented by Weglein et al., (1997).

However, a combination of the wavefield-decomposition technique and cross-correlation method can further identify and eliminate the source-side multiples.

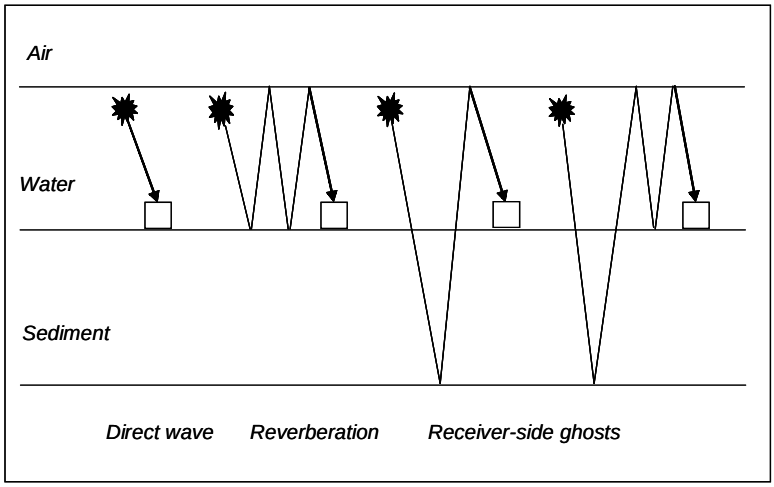

FIG. 23. Examples of downgoing waves in OBS data.

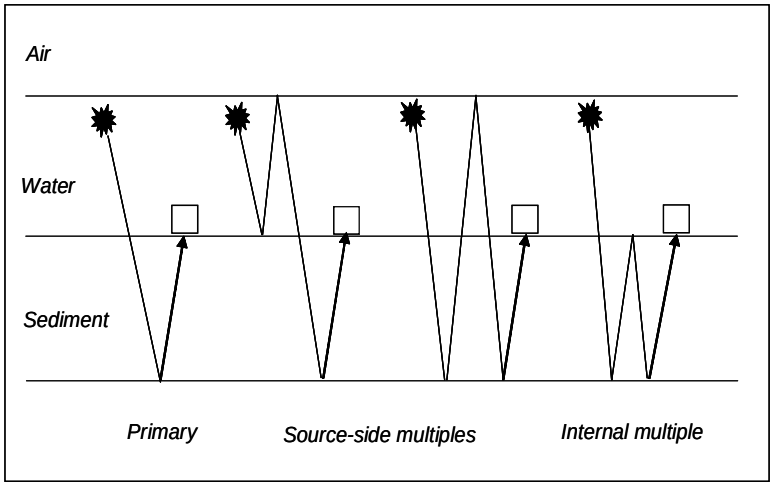

FIG. 24. Examples of upgoing waves in OBS data.

ACKNOWLEDGEMENTS

The support of the CREWES sponsors is most appreciated. Thanks to Chanpen Silawongsawat for the use of her modelling code and constructive discussions.

REFERENCES

Aki, K. and Richards, P.G., 1980, Quantitative seismology: W.H. Freeman and Co.

Amundsen, L. and Reitan, A., 1994, Decomposition of multicomponent sea floor data into upgoing and downgoing P- and S-waves: Geophysics **60**, 563-572.

Amundsen, L. and Reitan, A., 1995, Estimation of sea-floor wave velocities and density from pressure and particle velocity by AVO analysis: Geophysics **60**, 1575-1578.

Barr, F.J. and Sanders, J.I., 1989, Attenuation of water-column multiples using pressure and velocity detectors in a water-bottom cable: 59th Annual International SEG Meeting, Expanded Abstracts, 653-656.

Ball, V. and Corrigan, D., 1996, Dual-sensor summation of noisy ocean-bottom data: 66th Ann. Internat. Mtg., Soc. Expl. Geophys., Expanded Abstracts, 28-31.

Barr, F.J., Chambers, R.E., Dragoset, W. and Paffenholz, J., 1997, A comparison of methods for combining dual-sensor ocean-bottom cable traces: 67th Ann. Internat. Mtg., Soc. Expl. Geophys., Expanded Abstracts, 67-70.

Berg, E., Svenning, B., and Martin, J., 1994, SUMIC: Multicomponent sea-bottom seismic surveying in the North Sea: Data interpretation and applications: 64th Ann. Internat. Mtg., Soc. Expl. Geophys., Expanded Abstracts, 477-480.

Berkhout, A.J.,1982, Seismic migration, imaging of acoustic energy by wavefield extrapolations: Elsevier Science Publ. Co., Inc.

Brown, R. J., 1999, Towards a polarity standard for multicomponent seafloor seismic data: CREWES Research Report **11**, 237-253.

Brown, R.J. and Yan, Y., 1999, Suppression of water-column multiples in multicomponent seafloor data: Preliminary results and proposal: CREWES Research Report **11**, 311-321.

Gilbert, F. and Backus, G., 1966, Propagator matrices in elastic wave and vibration problems: Geophysics **31**, 326-332.

Osen, A., Amundsen, L., and Reitan, A., 1999, Removal of water-layer multiples from multicomponent sea-bottom data: Geophysics **64**, 838-851.

Schalkwijk, K.M., Wapenaar, C.P.A., and Verschuur, D.J., 1999, Application of two-step decomposition to multicomponent ocean-bottom data: Theory and case study: J. Seismic Exploration **8**, 261-278.

Silawongsawat, C. and Margrave, G.F., 1998, The phase-shift cascade method of elastic wavefield modeling: 68th Ann. Internat. Mtg., Soc. Expl. Geophys., Expanded Abstracts, 1807-1810.

Weglein, A.B., Araujo, G.F., Carvalho, P.M., and Stolt, R.H., 1997, An inverse-scattering series method for attenuating multiples in seismic reflection data: Geophysics **62**, 1975-1989.

White, J.E., 1965. Seismic wave radiation, transmission and attenuation. McGraw-Hill, Inc.